

STRUCTURAL INTEGRITY ASSESSMENT OF A MINE HOIST ROPE ATTACHMENT ELEMENT WITH A CRACK

PROCENA INTEGRITETA KONSTRUKCIONOG ELEMENTA SPOJNOG PRIBORA DIZALICE SA PRSLINOM

Originalni naučni rad / Original scientific paper
UDK /UDC:

Rad primljen / Paper received: 27.8.2020

Adresa autora / Author's address:

¹) University of Zenica, Faculty of Mechanical Engineering, Zenica, Bosnia and Herzegovina, email: kjosip@mf.unze.ba

²) University of Zenica, Institute 'Kemal Kapetanovic', Zenica, Bosnia and Herzegovina

³) Josip Juraj Strossmayer University of Osijek, Mechanical Engineering Faculty in Slavonski Brod, Slavonski Brod, Croatia, email: pekon@sfsb.hr

Keywords

- fracture mechanics
- SINTAP/FITNET procedure
- FEM
- rope attachment
- mine hoist

Abstract

Structural integrity assessment of an element (lifting plate) of a mine hoist rope attachment with a surface crack is performed using the SINTAP/FITNET method. Different geometries of a semi-elliptical crack and load intensities are investigated. Material properties data used in the procedure are experimentally determined via tensile and fracture tests. Finite element method is implemented for determination of stress intensity factors and a stress profile necessary for the calculations. Two approaches to the assessment, FAD (failure assessment diagram) and CDF (crack driving force) provided in SINTAP/FITNET procedure are implemented and compared.

INTRODUCTION

Hoisting systems in mining facilities are the key connection between production systems and surface material processing systems. Their continuous operation is necessary to achieve a production plan. An important part of a mine hoist is an attachment assembly between a rope and a cage, and a periodical inspection and replacement of the assembly parts is obligatory to satisfy safety regulations. When a discontinuity (e.g. crack) is detected in the material, structural integrity assessment should be based on crack tip parameters, i.e. applying fracture mechanics. In this paper, structural integrity of a part of a mine hoist attachment assembly in case of a crack appearance is investigated. Critical loads for different crack geometries are determined implementing SINTAP/FITNET procedure /1-3/.

ROPE ATTACHMENT ASSEMBLY AND LIFTING PLATE

The lifting plate, a part of the rope attachment assembly from Coal Mine Zenica, excavation 'Raspotočje' is considered in the investigation, Fig. 1. The rope is connected with a hearth shaped plate (pos. 7) using rope clumps. Load is

Ključne reči

- mehanika loma
- SINTAP/FITNET procedura
- MKE
- spojni pribor užeta
- dizalica

Izvod

Primenom SINTAP/FITNET metode procenjen je integritet konstrukcionog elementa spojnog pribora (poluga dizalice) rudarskog postrojenja dizalice sa površinskom prslinom. Istražene su različite geometrije polueliptične prsline i intenziteti opterećenja. Podaci o svojstvima materijala korišćeni u proceduri su eksperimentalno određeni putem ispitivanja na zatezanje i lom. Primenjena je metoda konačnih elemenata za određivanje faktora intenziteta napona i raspodele napona duž preseka, neophodnih za proračun. Primenjena i upoređena su dva pristupa u proceni, FAD (dijagram procene loma) i CDF (sila razvoja prsline), koji su dostupni u okviru SINTAP/FITNET procedure.

carried by means of parts that are interconnected using bolts secured with split pins (pos. 8-13). The assembly is designed following the regulation in /4/, with the required minimal safety factor of ten for the statical load of 211 kN. The design load is the sum of the weight of all structural parts, rope, and maximal cargo, /5, 6/. The rope attachment parts are made from standard structural steel, S355JR according to EN 10027-1 /5, 6/, with relevant mechanical properties given in Table 1.

MATERIAL TESTING AND PROPERTIES

Material properties (yield strength, tensile strength and fracture toughness) needed for the research are obtained from the experimental tests of the material, from the part disassembled at the mine facility, after extensive exploitation. Figure 2 shows the zone of the part from where the test specimens were cut out. Three specimens for tensile testing and four for fracture testing are made. Besides them, more specimens for different tests are also made /6/, but these tests are not considered here, because they are not used in the calculations presented in this paper.

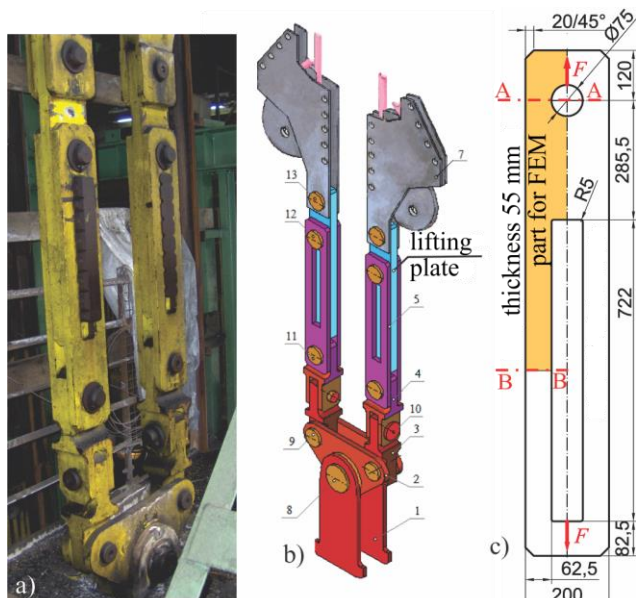


Figure 1. Rope attachment assembly: photo (a); CAD model (b); and lifting plate (c).

Table 1. Steel S355JR properties.

Elasticity modulus, E (GPa)	Poisson ratio, ν	Minimal yield strength, $R_{p0.2}$ (MPa)	Minimal tensile strength, R_m (MPa)
210	0.3	355	510

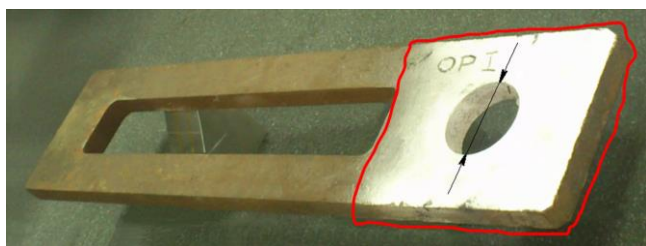


Figure 2. The part of lifting plate used for specimens.

Tensile test

Quasi-static tensile testing is performed according to BAS EN 6982 at temperature of 20°C, with the specimens having the dimensions as shown in Fig. 3. The universal Amsler tension tester with force up to 200 kN is used combined with the electronic extensometer (measuring range from 0.02 up to 2 mm, accuracy ± 0.001 mm).

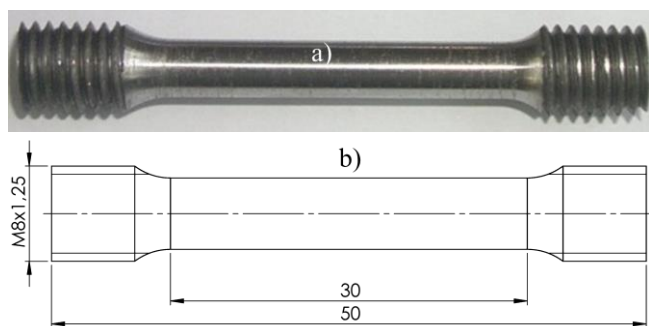


Figure 3. Tensile test specimen: photo (a); drawing (b).

A conventional stress-strain diagram for specimen 1 is shown in Fig. 4. Other specimens have shown similar stress-strain behaviour and test results.

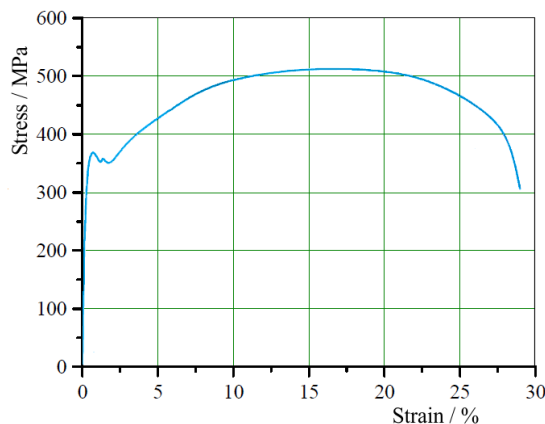


Figure 4. Stress-strain diagram for specimen 1.

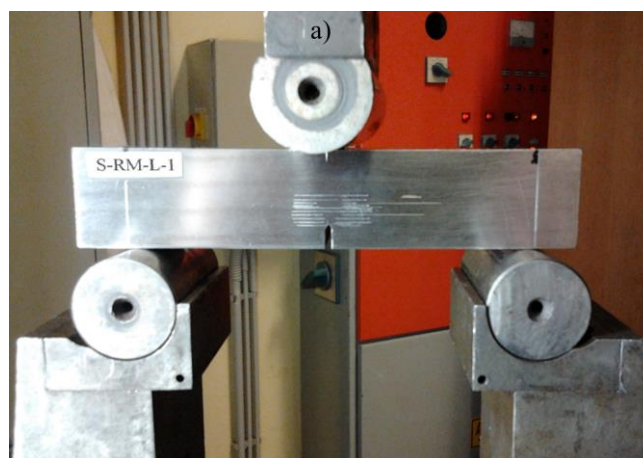
The test results for the three specimens together with the calculated mean values are given in Table 2. The test results did not show any noticeable weakening of the material (compare with Table 1).

Table 2. Tension tests results.

Specimen no.	$R_{p0.2}$ (MPa)	R_m (MPa)
1	371.4	532.0
2	360.3	540.9
3	359.3	540.2
Average	363.7	537.7

Fracture test

Fracture behaviour of the material is described using an R-curve (resistance curve) in terms of CTOD (Crack Tip Opening Displacement), /7/. Fracture testing is performed implementing multiple specimen methods according to the GKSS procedure /8/, using servo hydraulic testing machine (Instron 1255) under displacement control (stroke velocity 1 mm/min) at room temperature (+24°C), Fig. 5a. Four SEB (Single Edge Bend) specimens are made from the exploited material and prepared according to the ASTM standard /9/, with the dimension shown in Fig. 5b. All specimens are pre-cracked in three point bending fatigue according to the ASTM standard /9/ with the initial crack size of minimal 12 mm, being in the required range $0.45 < a_0/W < 0.65$.



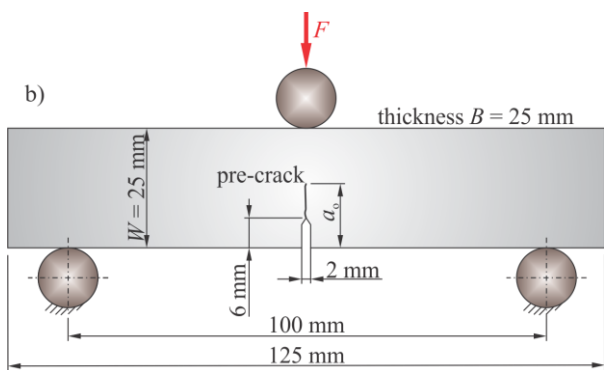


Figure 5. SEB specimen and fracture testing configuration: photo (a); drawing with loading scheme (b).

During fracture testing, CTODs are optically measured using ARAMIS GOM GmbH measuring system /10/. Black and white speckled pattern is applied to the specimen surfaces around the pre-crack for DIC (digital image correlation) measurement of a crack /11, 12/. The test results (CTOD vs. load) for the four specimens are shown in Fig. 6. The tests for the four specimens are completed with different final (maximal) CTODs in order to cover the range of the R-curve, according to the GKSS procedure.

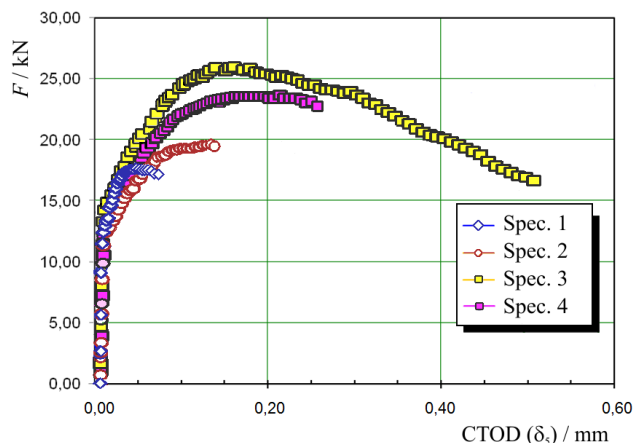


Figure 6. CTOD test results.

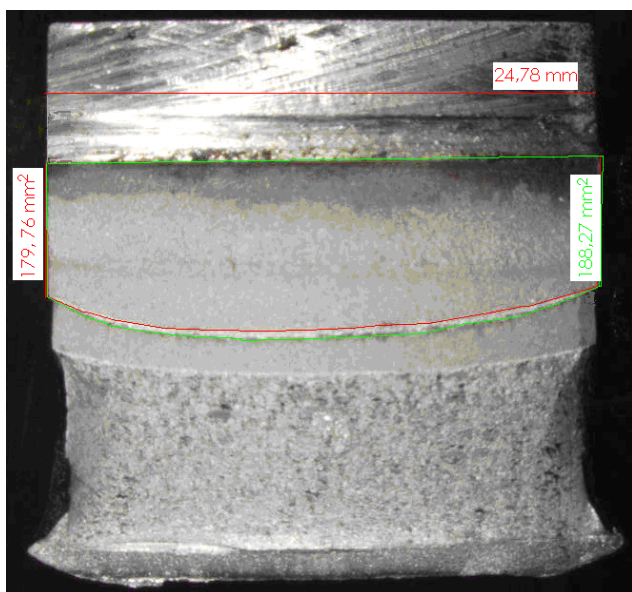


Figure 7. Crack area measurements for specimen 3.

After the test, the initial (fatigue) and final crack size (hence, and crack extensions) are calculated from the measured crack area using stereo microscope OLYMPUS SZX12 (Fig. 7 shows measurement results of specimen 3). Finally, the CTOD R-curve is constructed through the points of maximal crack extensions and CTODs for the four specimens, Fig. 8. The point of crack initiation /7, 8/ (see Fig. 8), δ_i , on the R-curve is taken as the CTOD fracture toughness of the material, δ_{mat} .

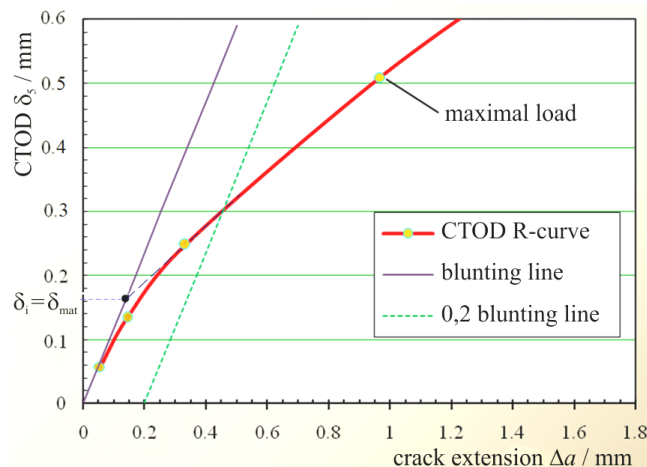


Figure 8. CTOD R-curve of the material.

Results of fracture toughness expressed obtained via previously described testing are in Table 3. Fracture toughness expressed in terms of stress intensity factor, K_{mat} , is calculated from δ_{mat} using a definition of CTOD from the strip-yield model, /7/:

$$K_{mat} = \sqrt{\delta_{mat} R_{p0.2} E} \quad (1)$$

Table 3. Fracture toughness testing results.

δ_{mat} (mm)	K_{mat} (MPa·m ^{1/2})
0.1614	111.0

There are different relations between K_{mat} and δ_{mat} (K and CTOD) available in literature, and the implemented one provided later excellent agreement between the results from the two SINTAP/FITNET assessment approaches, using as parameters K_{mat} and δ_{mat} (please see the following chapter and Figs. 13 and 14).

SINTAP/FITNET PROCEDURE

FITNET FFS procedure /2/ is used for structural integrity assessment in which the fracture mechanics module is formulated from SINTAP /3/, and both results are from the EU-funded projects. Hence, it is often referred to as the SINTAP/FITNET procedure /1/ (as in this paper). The procedure enables an assessment of component fitness-for-service ability in case of crack appearance. The assessment is possible with two approaches, the FAD (failure assessment diagram), or the CDF (crack driving force) analysis. Both analyses are harmonized with each other and should lead to identical conclusions, so the choice is a personal preference. Here, both analyses are used and compared.

The FAD assessment is based on the failure curve given as a function of L_r , the ligament yielding parameter:

$$K_r = f(L_r), \tag{2}$$

where: K_r is the crack driving force, and it is expressed in terms of K , the stress intensity factor; and K_{mat} is the fracture toughness of the material:

$$K_r = K / K_{mat}. \tag{3}$$

For the integrity assessment of the component, it is required to determine values of K_r and L_r (using element and crack geometry, load and material properties) and with it the position of the point in FAD with a failure curve. If a point is below a curve it is in the safe zone, and otherwise in a potentially unsafe zone.

The CFD assessment uses CDF functions for crack tip displacement, δ_e , given by:

$$\delta = \delta_e / [f(L_r)]^2, \tag{4}$$

with

$$\delta_e = K^2 / (E\sigma_Y), \tag{5}$$

where: E is elasticity modulus (for plane stress); and σ_Y is the material yield strength. Note that the $f(L_r)$ functions in Eqs.(2) and (4) are identical. The critical condition is reached when the value of CDF, Eq.(4), is identical or higher than the material fracture toughness, δ_{mat} . It is also possible to use CFD functions in terms of J-integral in the SINTAP/FITNET procedure, but it is not considered in this paper.

FEM ANALYSIS

A part of the parameters needed for the FINTET/SINTAP calculations are determined by FEM. Commercial software Ansys® /13/ is used to determine normal stress distribution without crack and stress intensity factor for different cracks in the cross section A-A (Fig. 1c). It is possible to simplify the numerical model and use only a part of the lifting plate in the simulations due to symmetry and uniform stress distribution in cross section B-B (Fig. 1c). Boundary conditions for the model in the numerical simulations are shown in Fig. 9a. Bearing load of 100 kN acting on the pin hole of the part is adopted as a minimal (base) for investigation and is used in FEM simulations. The surface semi-elliptical crack (Fig. 9b) is modelled in FEM crack analyses. Three different ratios of crack-to-cross section widths, $2c/w = \{0.25/0.5/0.75\}$, and for each - three different crack shapes defined by width-to-depth ratios, $a/c = \{0.5/1/2\}$ are simulated. Figure 10 shows FEM plots of normal stress plot and mode I stress intensity factor for one of the crack geometries. Obtained results of stress intensity factor for all considered crack geometries under the base load of 100 kN are given in Table 4. Stress intensity factors for higher load levels (200, 300 kN, ...) are calculated by multiplying the values for the base load of 100 kN with the ratio of actual load-to-base load (2, 3, ...) assuming linear behaviour. The assumptions are confirmed with several additional FEM simulations for randomly chosen higher load levels and crack geometries.

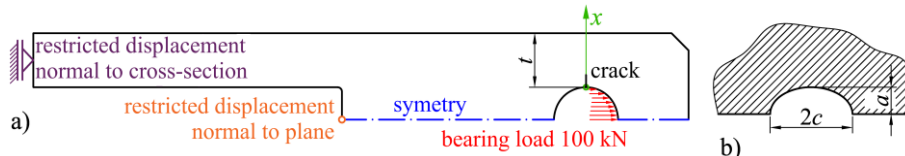


Figure 9. FEM model: boundary conditions (a); crack shape (b).

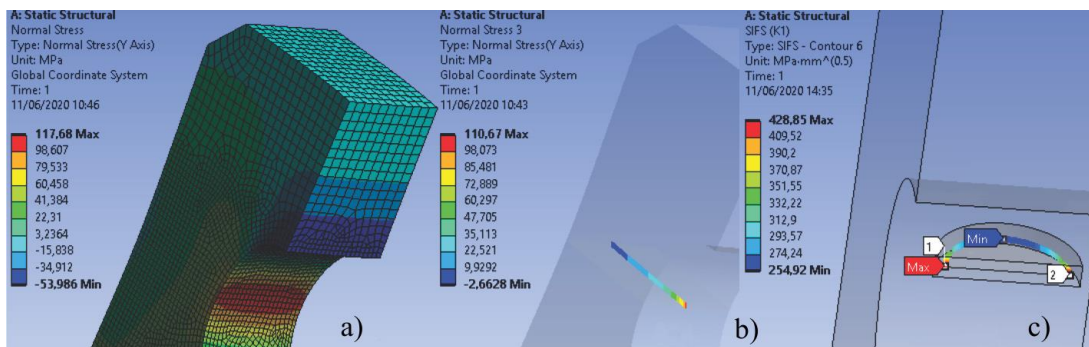


Figure 10. FEM results: normal stress plot (a); normal stress profile (b); stress intensity factor for a crack with the dimensions $c = 13.8$ mm and $a = 13.8$ mm (c).

Table 4. Stress intensity factors FEM results for different crack sizes.

c (mm)	6.9			13.8			20.6		
a (mm)	3.4	6.9	10.3	6.9	13.8	20.6	13.8	27.5	41.3
K_I (MPa·mm ^{1/2})	261.2	318.0	382.7	329.4	428.9	537.5	383.2	495.8	649.9

LIGAMENT YIELDING PARAMETER

A ligament yielding parameter is a key parameter for the accuracy of the SINTAP/FITNET procedure. It is defined as the ratio of a part load F with the net section yield load (also called limit load) F_Y , or its connected stress parameters, referent stress σ_{ref} and yield stress σ_Y :

$$L_r = F / F_Y = \sigma_{ref} / \sigma_Y. \tag{6}$$

Definition of parameters in Eq.(6) is based on the determination of a load or stress when a part starts to behave with pronounced nonlinearly. It is studied in many papers and different solutions are proposed, /1/. The solution for the appropriate substitutive geometry, a surface crack in a

plate (Fig. 11), is implemented here /14/. The ligament yielding parameter is calculated by using:

$$L_r = \frac{g \frac{\sigma_b}{3} + \sqrt{g^2 \frac{\sigma_b^2}{9} + (1-\zeta)^2 \sigma_m^2}}{(1-\zeta)^2 \sigma_Y}, \quad (7)$$

with $g = 1 - 20\zeta^3 \left(\frac{a}{2c}\right)^{0.75}, \quad \zeta = \frac{a \cdot 2c}{t(2c+2t)}.$

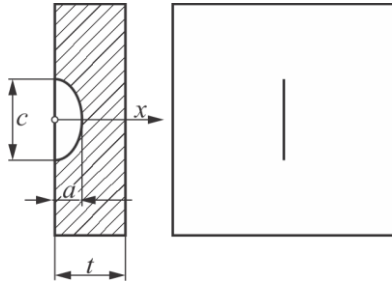


Figure 11. Substitutive crack geometry - surface crack in a plate.

Stress profile values, the bending stress σ_b and membrane stress σ_m , are calculated using FEM results, as presented in the following section.

Stress profile

The implemented solutions for L_r require a definition of linear stress profile in a form of:

$$\sigma_{lin} = \sigma_m + \sigma_b \left(1 - \frac{2x}{t}\right). \quad (8)$$

The stress profile (Fig. 12) is expressed in a form of a fifth-order polynomial from the FEM results (Fig. 10b) for 100 kN of load by regression:

$$\begin{aligned} \sigma_{(100\text{ kN})} = & 110.19 - 514.7 \left(\frac{x}{t}\right) + 1415.3 \left(\frac{x}{t}\right)^2 - \\ & - 2207.1 \left(\frac{x}{t}\right)^3 + 1752.5 \left(\frac{x}{t}\right)^4 - 559.3 \left(\frac{x}{t}\right)^5. \end{aligned} \quad (9)$$

Membrane and bending stress values can be calculated with the integrals, /1/:

$$\sigma_m = \frac{1}{t} \int_0^t \sigma dx, \quad \sigma_b = \frac{6}{t^2} \int_0^t \sigma \left(\frac{t}{2} - x\right) dx. \quad (10)$$

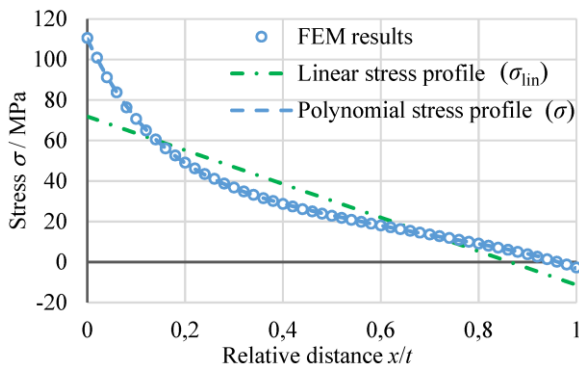


Figure 12. Stress profiles.

Values of 30.29 and 41.57 MPa for membrane and bending stress, respectively, are obtained by integrating Eq.(9).

For higher load levels (200, 300 kN, ...), the stress values for base load of 100 kN are multiplied with the ratio of actual load-to-base load (2, 3, ...) assuming linear behaviour.

FAILURE CURVE

SINTAP/FITNET procedure /1-3/ offers different options for definition of $f(L_r)$ depending on available data on material properties. The standard option 1 is used when the yield strength and the ultimate tensile strength from the material tests are available, as is the case in this paper. There are two variants, A and B, for option 1, depending on whether the material is expected to display a yield plateau or not, in respect. Here, option 1B is used, providing a more conservative estimate defined by:

$$f(L_r) = \frac{0.3 + 0.7 \exp(-\mu L_r^6)}{\sqrt{1 + 0.5 L_r^2}} \quad \text{for } 0 \leq L_r \leq 1 \quad (11)$$

$$f(L_r) = f(L_r = 1) \cdot L_r^{\frac{N-1}{2N}} \quad \text{for } 1 \leq L_r \leq L_{r\text{max}}$$

Variables in Eq.(11) are calculated with:

$$\mu = \min \left\{ \begin{array}{l} 0.001(E / R_{p0.2}) \\ 0.6 \end{array} \right., \quad (12)$$

$$N = 0.3 \left(1 - \frac{R_{p0.2}}{R_m} \right). \quad (13)$$

Maximal value of L_r represents the point of plastic collapse and is given by:

$$L_r^{\text{max}} = \frac{R_{p0.2} + R_m}{2R_{eL}}, \quad (14)$$

with $R_{eL} = 0.95R_{p0.2}$.

CDF RESULTS

Results of structural integrity assessment of the lifting plate with a surface crack by CDF approach are shown in Fig. 13. Different crack geometries and load levels are analysed. All aspects of the procedure are explained in previous chapters. According to the CDF, the first point in the unsafe zone is for the 500 kN of force and for maximal crack dimensions. At smaller crack dimensions, the critical loads are in the range from 600 to 800 kN.

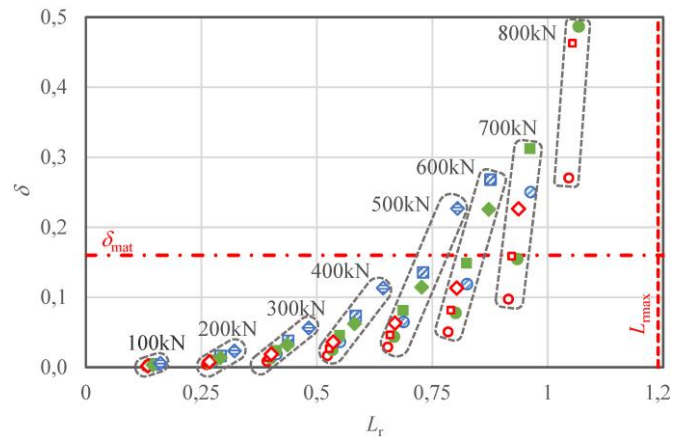


Figure 13. CDF results.

The following legend is applicable to both Figs. 13 and 14:

- $c/a=2, 2c/w=0,25$
- $c/a=2, 2c/w=0,5$
- ◐ $c/a=2, 2c/w=0,75$
- ◑ $c/a=1, 2c/w=0,25$
- $c/a=1, 2c/w=0,5$
- ◒ $c/a=1, 2c/w=0,75$
- ◓ $c/a=0,5, 2c/w=0,25$
- ◔ $c/a=0,5, 2c/w=0,5$
- ◕ $c/a=0,5, 2c/w=0,75$

FAD RESULTS

Results of structural integrity assessment of the lifting plate with a surface crack by FAD approach are shown in Fig. 14. The results show excellent agreement with CDF results, hence confirming the harmonization of the two approaches in SINTAP/FITNET, and also the calculation procedures done in this paper.

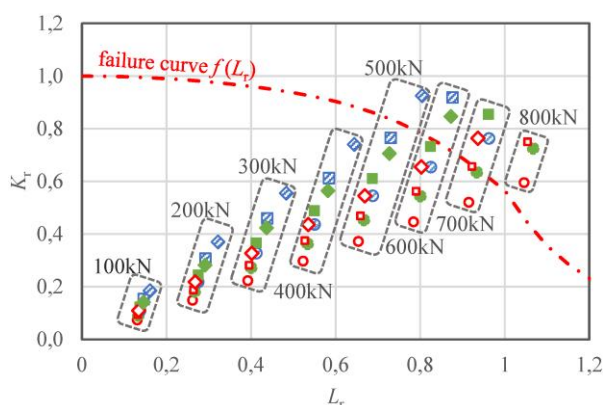


Figure 14. FAD results.

RESULTS ANALYSIS

Critical conditions obtained with the FAD or CDF philosophy show very high values for a load intensity or a crack size. The critical force values in case of a crack appearance are several times larger than the design load for the element. This is expected since a high safety factor is used in the design of this type of structure (mining facilities). Application of partial safety factors, or reserve factors is provided in SINTAP/FITNET, and they should be considered and implemented in further research, leading to practical guidelines regarding structural integrity assessment of a component in a mine hoist attachment assembly in case of a crack appearance.

REFERENCES

- Zerbst, U., Schödel, M., Webster, S., Ainsworth, R.A., Fitness-for-Service Fracture Assessment of Structures Containing Cracks - A Workbook based on the European SINTAP/FITNET Procedure, Academic Press, 2007.
- Koçak, M., Webster, S., Janosch, J.J., et al., Fitness for Service Procedure (FITNET), Revision MK8, GKSS Research Center, 2008.
- SINTAP: Structural INTEgrity Assessment Procedure for European Industry, Final Revision, EU Project BE 95-1462, BRITE-EURAM Programme, 1999.

- Pravilnik o tehničkim normativima pri prevozu ljudi i materijala oknima rudnika (*Regulations on technical norms in people and material transport in mine shafts*) (in Serbian), Tehnički propisi, Rudarstvo, Belgrade, 1986, pp.490-526.
- Hadžalić, M., Razvoj algoritama za određivanje integriteta i vijeka trajanja strukturalnih elemenata izvoznih postrojenja, (*Development of algorithm for structural and life assessment of mine hoist components*) (in Bosnian), PhD Thesis, University of Zenica, Faculty of Mechanical Engineering, Zenica, Bosnia and Herzegovina, 2018.
- Dopunski rudarski projekat za izradu i rekonstrukciju dvoetažnog izvoznog koša i pripadajućih spojnih pribora na izvoznom oknu 'Raspotočje', RI Tuzla, 1984. (in Bosnian: *Annex of mining project for construction and reconstruction of 2-deck conveyance cage and associated connecting components at shaft hoist 'Raspotočje'*).
- Anderson, T.L., Fracture Mechanics, Fundamentals and Applications, 3rd Ed., CRC Press, 2005. doi: 10.1201/9781420058215
- Schwalbe, K.-H., Heerens, J., Zerbst, U., et al., EFAM GTP 02 - The GKSS test procedure for determining the fracture behaviour of materials, GKSS-Forschungszentrum Geesthacht GmbH, 2002.
- ASTM E1820-01, Standard Test Method for Measurement of Fracture Toughness, ASTM Int., West Conshohocken, PA, 2001. www.astm.org
- ARAMIS GOM GmbH. www.gom.com
- Paolinelli, L.D., Carr, G.E., Gubeljak, N., et al. (2013), Fracture toughness analysis of a ductile steel by means of 3D surface displacements, Eng. Fract. Mech. 98: 109-121. doi: 10.1016/j.engfracmech.2012.12.006
- Čolić, K., Burzić, M., Gubeljak, N., et al. (2017), Digital image correlation method in experimental analysis of fracture mechanics parameters, Sci. Tech. Rev. 67(2): 47-53. doi: 10.5937/str1702047C
- Ansys Mechanical 2020, ANSYS Inc., www.ansys.com
- Al Laham, S., Stress Intensity Factor and Limit Load Handbook, EPD/GEN/REP/0316/98, British Energy Generation Ltd, 1998.

© 2021 The Author. Structural Integrity and Life, Published by DIVK (The Society for Structural Integrity and Life 'Prof. Dr Stojan Sedmak') (<http://divk.inovacionicentar.rs/ivk/home.html>). This is an open access article distributed under the terms and conditions of the [Creative Commons Attribution-NonCommercial-NoDerivatives 4.0 International License](https://creativecommons.org/licenses/by-nc-nd/4.0/)